

# Soil and Rock Classification from Pressuremeter Data. Recent Developments and Applications. Classification pressiométrique des sols et des roches. Développements récents et applications.

J.-P. Baud

*Eurogé, Avrainville, France, baud@eurogeo.fr*

**ABSTRACT:** A chart classification of soils and rocks derived from classical Ménard Pressuremeter parameters  $p_{LM}^*$ ,  $E_M$  and earth pressure at rest  $p_0$ , was previously proposed (Baud & Gambin, 2013), linked to the alpha ( $\alpha$ ) rheological coefficient defined by Ménard (1961).

The reliability of this (Pressiorama<sup>®</sup>) classification for describing soil layers was tried in various case histories, and checked by several authors in recent years (ref. in the paper).

In this paper we indicate development of the Pressiorama classification in four trends:

- Adaptation of coefficient  $k_E$  in the expression of  $\alpha$ , taking into account some site conditions and drilling quality as experimented in these case histories.
- Correlation between this Pressiorama classification and the behaviour of soils and rocks in terms of auger-drilling (refusal level), drilling (drillability), driving (drivability) and even jetting. A graphical chart ( $E_M/p_0$ ,  $\alpha$ ) is proposed.
- How to use Pressuremeter data sets  $\{E_M, p_{LM}^*, p_0\}$  on one site to determine seismic zoning according to Eurocode 8 (EN 1998) as a substitute to the parameters  $C_u$  (shear stress) and  $V_s$  (seismic velocity), the main criteria proposed by this Standard, but less easy to obtain during soils surveys than pressuremeter data. The proposal is based on two classic relations,  $C_u = f(p_{LM}^*, \alpha)$  and  $V_s = f(E_M, \alpha, \gamma_h, g)$ , allowing to define soil seismic class only from  $E_M$ ,  $p_{LM}^*$ , and PMT tests depths.
- Proposition of a new graph [ $E_{c1}/E_M$ ;  $p_{LM}^*/p_0$ ] by using one-cycle PMT.

**Keywords:** Pressuremeter, Ménard modulus, Drillability, Soil classification, Seismic zoning.

**RÉSUMÉ :** Un abaque de classification des sols et des roches, basé sur les paramètres classiques issus du Pressiomètre Ménard  $p_{LM}^*$ ,  $E_M$  et la pression des terres au repos  $p_0$  au niveau de l'essai, a été proposé (Baud & Gambin 2013), intégrant le coefficient rhéologique  $\alpha$  (alpha) de L. Ménard (1961).

La fiabilité de cette classification (Pressiorama<sup>®</sup>) pour décrire la lithologie des sols a été testée sur différents chantiers par l'auteur, et également par différents auteurs publiés récemment (réf. dans l'article).

L'article montre le développement de cette classification dans différentes applications :

- Adaptation du coefficient  $k_E$  dans l'expression de  $\alpha$ , prenant en compte les conditions de site ressortant de ces applications publiées ou non.
- Corrélation entre cette classification et le comportement des sols et roches en termes de refus à la tarière, de forabilité, de battage et vibrofonçage. Une expression graphique est proposée en surimposition sur le diagramme ( $E_M/p_0$ ,  $\alpha$ ).
- Utilisation des données pressiométriques  $\{E_M, p_{LM}^*, p_0\}$  d'un site pour déterminer le zonage sismique en remplacement des paramètres proposés par l'Eurocode 8 (EN 1998),  $C_u$  (résistance au cisaillement) et  $V_s$  (vitesse sismique), données moins courantes sur site que les données pressiométriques. La proposition est basée sur deux relations classiques,  $C_u = f(p_{LM}^*, \alpha)$  et  $V_s = f(E_M, \alpha, \gamma_h, g)$ , permettant de caractériser un site avec les seules valeurs de  $E_M$ ,  $p_{LM}^*$ , et la profondeur des essais.
- Proposition d'un nouvel abaque [ $E_{c1}/E_M$  ;  $p_{LM}^*/p_0$ ] utilisant les résultats de l'essai pressiométrique à un cycle.

**Mots-clés :** Pressiomètre, module Ménard, Forabilité, Classification des sols, Zonage sismique.

## 1. Introduction

The concept of sorting pressuremeter results by consolidating homogeneous subsets, before giving a statistical value to averages and dispersions of results, led to the creation of specific charts. Due to the characteristic typology of pressuremeter tests depending on the

behaviour of ground subject to the test of cylindrical expansion, these charts become naturally soil and rocks classification modes. The interest is to furnish direct estimation for a lot of properties, more or less directly correlated to PMT measurements, such as elastic modulus hypothesis, refusal and drillability prediction, shear stress, seismic velocity, or estimation of liquefaction risk.

## 2. Use of PMT Pressiorama charts

### 2.1. An image of the spectrum of soil heterogeneity, and diversity of geotechnician's approach

The Pressiorama diagram as proposed originally (Baud, 2005) basically consists to report, from a series of PMT from one site survey,  $p^*_{LM}$  values versus  $E_M/p^*_{LM}$  ratio. Subsequently, various amendments have been added: extension to rocks domain, value for  $\alpha$  rheological coefficient, replacement of  $p^*_{LM}$  by pressuremeter state parameter  $p^*_{LM}/p_0$  (Baud & Gambin, 2011, 2013, 2016). The concept of pressuremeter state parameters was suggested by Dupla & Canou (2005). In the same time, several authors published case histories by using the diagram in various soils and rocks throughout different sites in the world:

- Ritsos *et al.* (2013) show on different geological formations in Greece a good correlation for cohesive and granular zones.
- Reiffsteck *et al.* (2013) point more dispersion, on the site of Grand Paris survey, by reporting pressuremeter surveys from a lot of drilling companies; they propose to modify the presentation of PMT parameters by using the axes [ $\alpha$  |  $p^*_{LM}/p_0$ ].
- Monnet (2013) resumes his theory of complete expression of  $p^*_{LM}$  as a function of friction angle  $\varphi'$ , dilatancy  $\psi$ , horizontal pressure  $K_0\gamma z$ , shear modulus  $G_e$  (rather than  $E_M$ ). He proposes to dispatch classification in 2 diagrams, [ $G_e/p_0$  |  $p^*_{LM}/p_0$ ] for granular soils, [ $\ln(G_e)$  |  $p^*_{LM}$ ] for cohesive soils.
- Kanji M.A. (2014) cites Pressiorama chart in a general review on soft rocks. One of his diagram of case histories for natural rocks, reporting correlation for compression strength UCS versus E50 modulus, can be directly compared to Pressiorama chart.
- Tarnawski *et al.* (2015) report a lot of tests results in the same graph, from different formations in Poland, and find rather difficult to differentiate them, pointing also the influence of test quality on  $E_M/p^*_{LM}$  ratio.
- Elfatih *et al.* (2015) make a statistical study of PMT results in one single lithology, the Nubian sandstone formation in Sudan, and show the evolution of PMT values for this weak rock correlative with weathering.
- Hamdi & Holeyman (2016) apply their numerical modelling of cylindrical cavity expansion to a rock mass under different stages of weathering, and report this evolution in Pressiorama compared with PMT results on natural rocks.
- Marti, Perez & Devincenzi. (2019) study PMT surveys in Madingo, Cretaceous marly formation in Congo, and consider the ratio  $p^*_F/p^*_{LM}$  together with Pressiorama chart.

## 2.2. PMT State Parameters

Use of the limit pressure  $p^*_{LM}$  as main x-axis in the first Pressiorama is a natural way of thinking, as long as the concept of failing pressure in soils remains as one of the major contributions of Louis Ménard to geotechnical engineering. Unlike other parameters measured by different methods, for any soil-structure interaction, the failure criterion remains in direct proportion to the average limit pressure of the relevant area of soil. So, the range of values from 0 to 10 MPa for  $p^*_{LM}$  is by itself a classification of ground resistance from loose soils to soft rocks.

Nevertheless, for use as absolute soil classification, and for deducing intrinsic properties of soils, it is necessary to report PMT values to horizontal containment pressure  $p_0$  created by test depth, and consider all charts in terms of the adimensional pressiometric state parameters:  $p^*_{LM}/p_0$ ,  $E_M/p_0$ ,  $E_M/p^*_{LM}$ .

### 2.3. Adaptation of the expression for $\alpha$ coefficient to site conditions

In the expression of  $\alpha$  rheological coefficient, as given to draw parallel lines in Pressiorama chart (Baud & Gambin, 2013), we were brought to use a  $k_E$  "constant":

$$\alpha = \frac{\left(\frac{E_M}{p^*_{LM}}\right)^{\frac{1}{2}}}{k_E \cdot \left(\frac{p^*_{LM}}{p_0}\right)^{\frac{1}{4}}} \quad (1)$$

with a mean value of  $k_E=4$ , with lack of sufficient case histories experience at that moment.

Taking in consideration results from different authors cited above, and several recent case histories analysis (Baud *et al.*, 2018), it seems necessary that  $k_E$  could be slightly variable, from around 5 for minimum value of  $E_M/p^*_{LM}$ , to 3 for higher existing values of this parameter. So  $k_E$  is given as

$$k_E = (\pi + 2) / (\ln E_M/p^*_{LM})^{1/3} \quad (2)$$

At the same time, the exponents of the two dimensionless parameters was slightly modified, their ratio remaining the same, and the expression was proposed for rather "perfect" tests, considered as selfbored. For the cases where a given amount of "remoulding", or more often simply decompression due to time between drilling and placing the probe, occurs, a correction is needed.

A more accurate expression for  $\alpha$  is now given as:

$$\alpha = \frac{\left[\left(\frac{E_M}{p^*_{LM}}\right) \cdot \ln\left(\frac{E_M}{p^*_{LM}}\right)\right]^{\frac{1}{3}}}{(1-d) \cdot (\pi+2) \cdot \left(\frac{p^*_{LM}}{p_0}\right)^{\frac{1}{6}}} \quad (3)$$

Where " $d$ "  $< 1$ , is an estimation for decompression state of the soil before beginning of the test. This value can be either estimated by a knowledge of timing of drilling and testing sequences and drilling fluid used, or "measured" by the position of the point of contact between probe and borehole wall, in terms of volume (or radius) and pressure. So we can use to set an average value of " $d$ " for a test or series of tests the relation in the graph below (Fig.1).

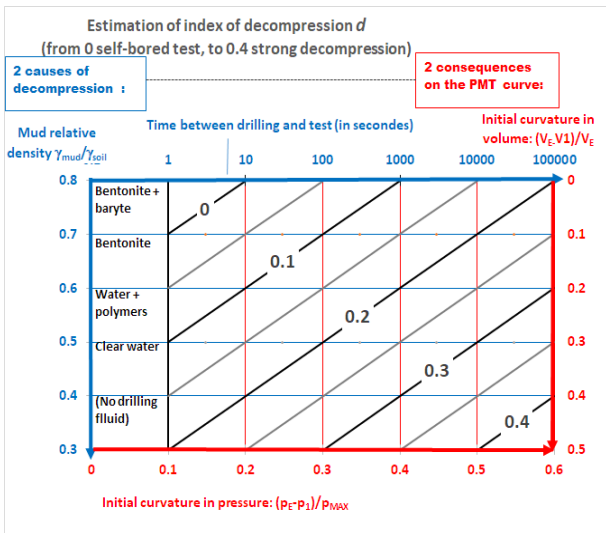
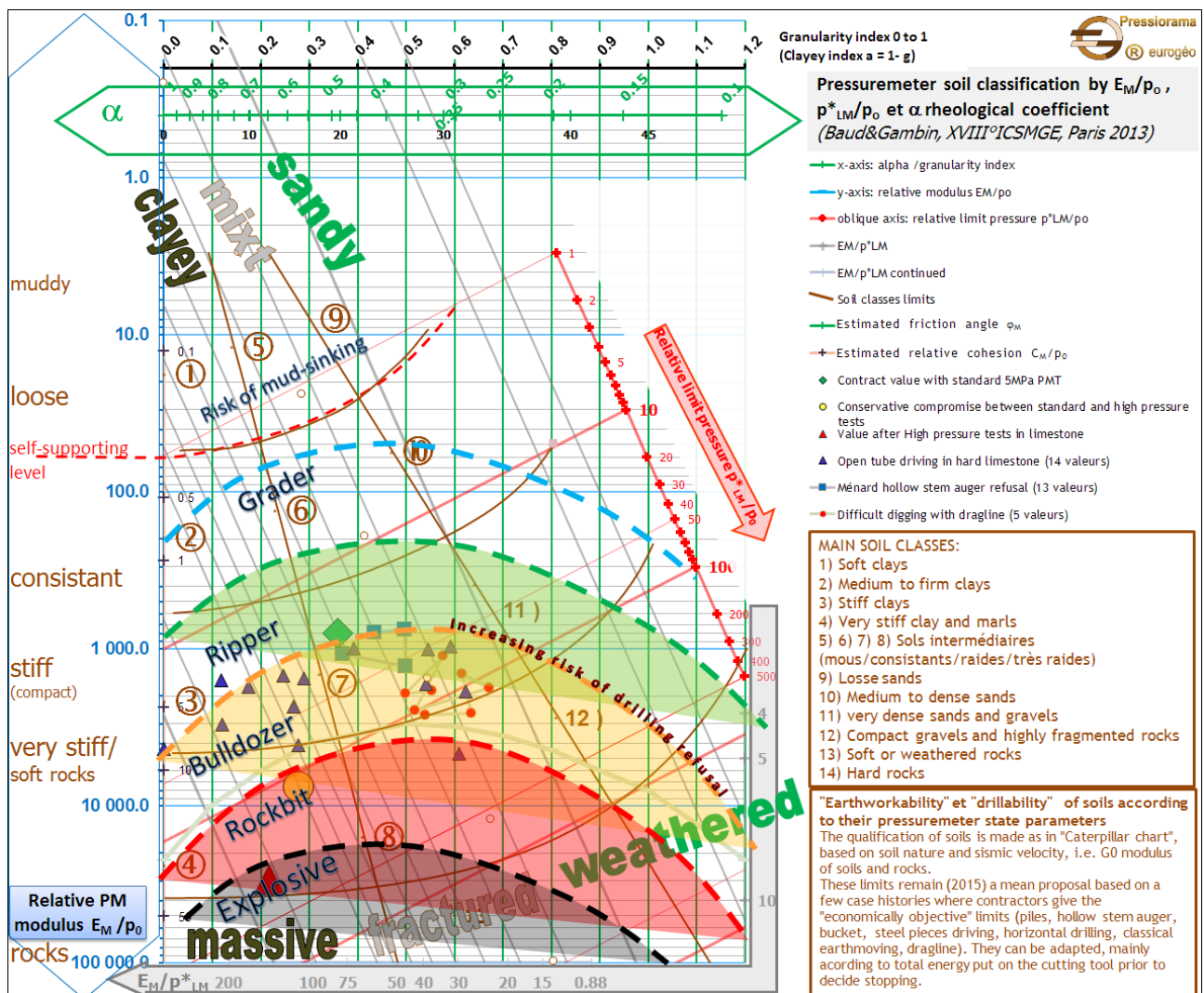


Figure 1. Estimation of the degree of decompression  $d$ , from 0 for a fully undecompressed test (self-boring pressuremeter) to 0.4 for a test in highly decompressed or remoulded soil.

### 3. PMT drillability chart



A series of case histories from different sites were examined, based on the experience of contractors in sinking, piling, driving, earthworks, often with a pressuremeter survey motivated by drilling, piling, driving or excavation conditions more difficult than hoped. By reporting these experiences in the Pressiorama graph as proposed (Baud & Gambin, 2013) with  $E_M / p_0$  on the ordinate (bottom positive) and on the abscissa  $\alpha$  value obtained from the test by Eq. 3, we can approximate on the diagram a succession of boundaries linked to the increase in the resistance of the soil or the rock to the working tool used (Fig. 2). These limits can be qualified by the nature of the machines or techniques commonly used in earthworks (grader, ripper, dozer, rockbit/rock-tooth or explosives). The result is similar to the "Seismic Velocity Charts" for rippers (Caterpillar®), based on the values of seismic velocity  $V_s$ , the proportionality of which is well known with the modulus of the soil or the rock. The refusal to auger drilling, a fairly general concept whatever the drilling rig, corresponds well enough to the border between soils, even very hardened, where a ripper can be used, and weathered or soft rocks where use of bulldozer is economically preferable.

Figure 2. Drillability chart from Pressuremeter tests.

#### 4. Eurocode 8 seismic zoning with PMT

This Standard enjoins geotechnicians to furnish a classification of building sites, based on geomechanical properties of the soil on the first 30 m of a site. Three parameters only are retained in the present redaction of the standard: seismic velocity  $V_{s,30}$  (m/s), NSPT, shearing resistance  $C_u$  (kPa). A table in Eurocode 8 indicates conventional limits for these parameters to define 5 seismic classes A to E, and 2 classes S1 S2. This table is an implicate correlation between  $V_s$  and  $C_u$  such as  $V_s$  (m/s) = 2  $C_u$  (kPa) (Fig. 3).

More often than not, in Europe, geotechnical surveys don't measure any of these three parameters. Instead, it can be proposed that mean results of a pressuremeter survey can be used by improved correlations of strength parameters  $p_{LM}^*$  to  $C_u$ , and deformation parameter  $E_M$  to  $V_s$ , by the way of using  $\alpha$  coefficient deduced from PMT by Eq. (3).

The 2 axes of the graph becomes :

- For y-axis, the relation  $C_u = p_{LM}^* / \beta$  (Ménard, 1963, Amar et al. 1991) where  $5 < \beta < 15$  according to soil nature, is generalised to any test with the assumption  $\beta \approx 5/\alpha$ , so:

$$C_u (S_u) = \frac{\alpha \cdot p_{LM}^*}{\pi + 2} \quad (4)$$

- For x-axis  $V_s$ , the classical relation  $G_0 = \rho \cdot V_s^2$  [ $\rho$  volumic mass deduced from estimation of  $\gamma$  ( $\gamma_h = \rho \cdot g$ )], and  $G_0 \approx 3 \cdot E_M / \alpha^2$  gives :

$$V_s (m/s) = \left[ \frac{3 \cdot g (m/s^2) \cdot E_M (kN/m^2)}{\gamma_h (kN/m^3) \cdot \alpha^2} \right]^{1/2} \quad (5)$$

A set of PMT representative results from 30m depth boreholes, as recommended by the standard, can be used in a ( $V_s, S_u$ ) graph as in Fig.3 to determine seismic class for a site.

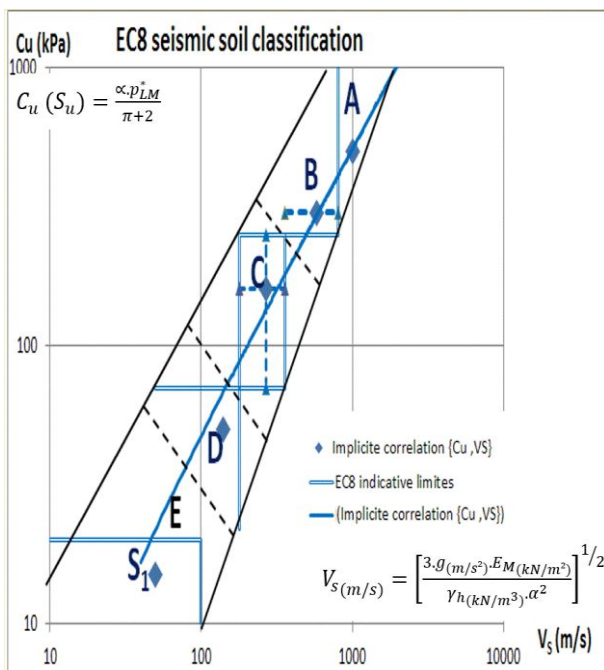


Figure 3. Use of Pressuremeter correlations for EC8 seismic soil classification [ $V_s$  |  $S_u$ ].

#### 5. Adimensional Pressiorama Chart.

The use of pressuremeter state parameter  $p_{LM}^*/p_0$  instead of  $p_{LM}^*$  as abscissa leads to a slightly different clouding of points corresponding to each of pressuremeter tests. In this normalized chart [ $p_{LM}^*/p_0$  |  $E_M/p_{LM}^*$ ] in logarithmic axes, Eq. (3) is used to draw in the cartesian plane  $\alpha$  values which appear as quasi linear (Fig. 5). The boundaries of the chart are: upwards (high values of  $E_M/p_{LM}^*$ ) the line  $\alpha = 1$ ; downwards, the line  $E_M/p_{LM}^* = 3$  below which no pressuremeter test is possible; to the right, the abscissa is limited to  $p_{LM}^*/p_0 = 1000$  and could if necessary be opened further, in the case of tests in rocks with a very high rupture pressure. The chart covers the full range of pressuremeter tests in soils; the upper limit for  $\alpha = 1$  is used to graduate a third axis for  $E_M/p_0$ , and can be indexed in terms of soil softness or resistance, from mud to hard soils, and indicate transition to HSSR (Hard Soils and Soft Rocks) and beyond to hard rocks.

Pressuremeter state parameters used in this adimensionnal chart should in the same way allow estimations for friction angle  $\phi'$  from PMT, which are included in the theoretical expressions given, among others, by Salençon (1966), Combarieu (1996) and Monnet (1997).

For now, we only propose to use the simplified expression of  $\phi'$  given by Ménard (TLM 1963) and Gambin (1977):

$$p_{LM}^* (bar) = k \cdot 2^{(\phi' - 24^\circ)/4} \quad (6)$$

with  $2 < k < 3$ , or 2.5 as a mean.

We proposed a generalisation of this classical relation as follows (Baud, 2016):

$$\frac{p_{LM}^*}{p_0} = b \cdot \alpha^c \cdot e^{\phi'/a} \quad (7)$$

whose parameters have been set, based on published friction angle measurement data  $a=6$ ,  $b=1/9$  and  $c=2$ :

$$\frac{p_{LM}^*}{p_0} = \frac{\alpha^2}{9} \cdot e^{\phi'/6} \quad (7bis)$$

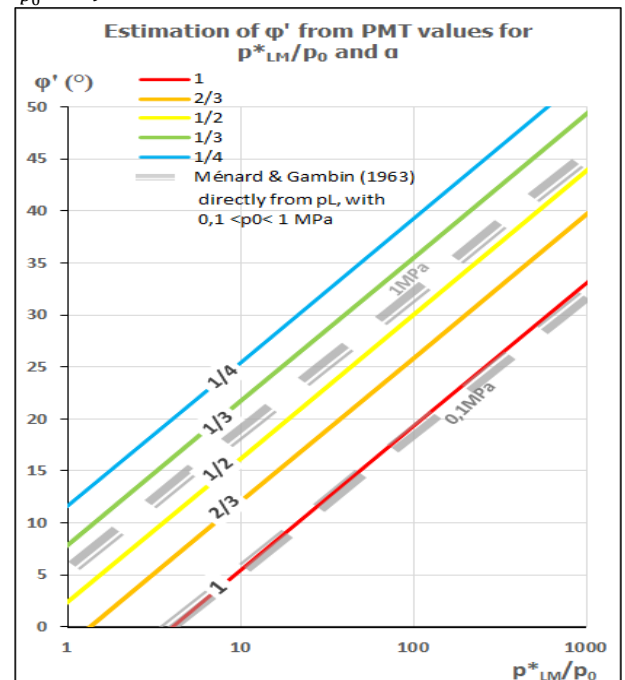


Figure 4. Estimation of  $\phi'$  from Pressuremeter test.

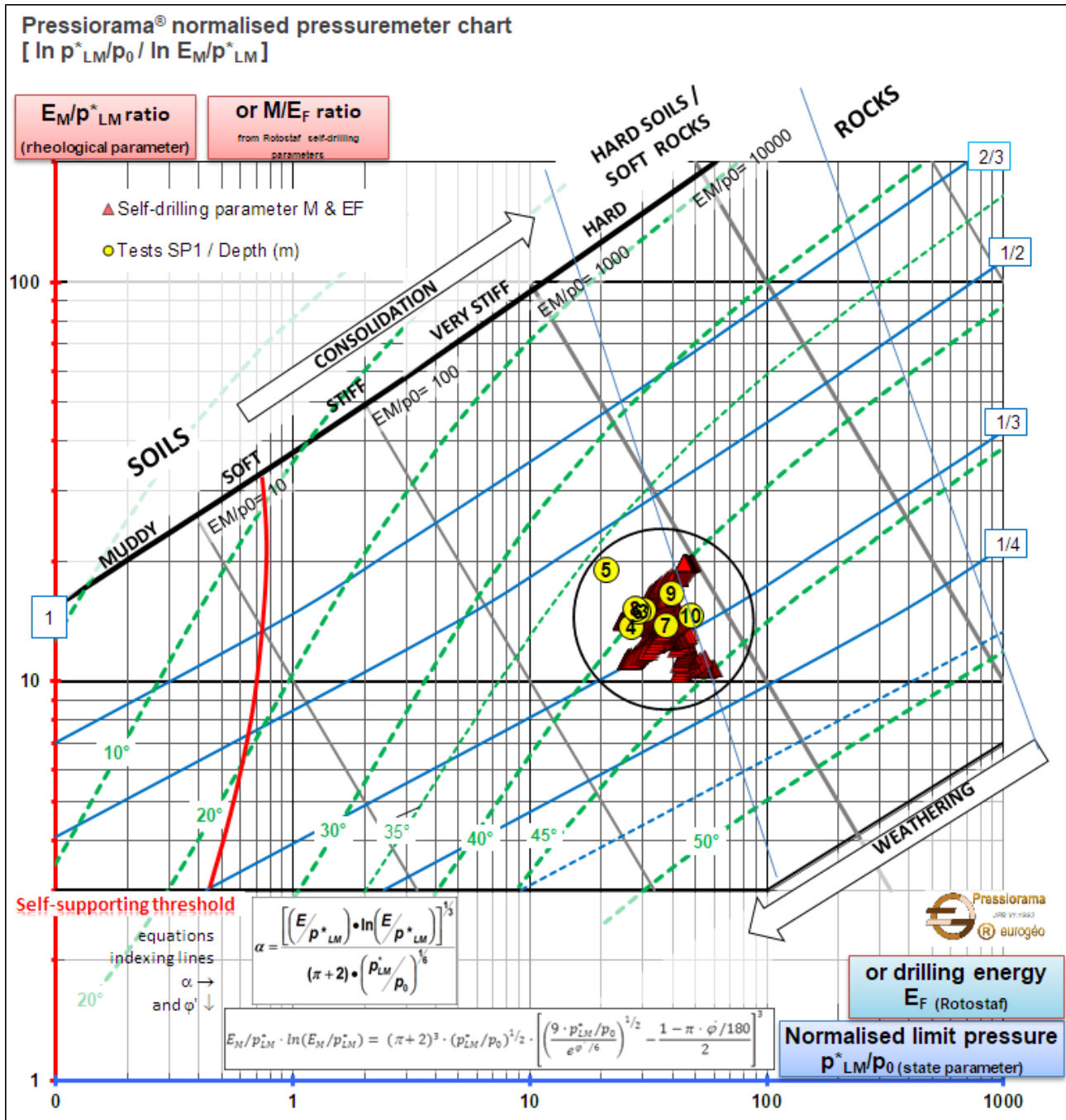
So let be a direct expression of friction angle:

$$\varphi' = 6 \cdot \ln \left[ \frac{9}{\alpha^2} \cdot \frac{p_{LM}^*}{p_0} \right] \quad (8)$$

The result can be compared to original proposition of Ménard and Gambin (Eq.6), from only  $p_{LM}^*$  (Fig. 4).

$$\varphi' = 3 \cdot \ln \left( \frac{9}{\alpha^2} \cdot \frac{p_{LM}^*}{p_0} \right) + \frac{90 \cdot (1-\alpha)}{\pi} \quad (9)$$

This allows us to draw lines of  $\varphi'$  values in the adimensional chart (Fig.5) as a function of  $p_{LM}^*/p_0$  and  $\alpha$ , the rheological coefficient,  $\alpha$  being itself a function of  $E_M$ ,  $p_{LM}^*$  and  $p_0$  according to Eq.3.



This result is consistent with the behaviour of sub-consolidated and normally consolidated soils, to get a reasonable approximation of  $\varphi'$  from a single standard Ménard pressuremeter test. However, the value of angle  $\varphi'$  thus established obviously quickly becomes too high as consolidation ( $E_M / p_{LM}^*$  or  $E_M / p_0$ ) progresses, and would lead to values greater than 45° for any overconsolidated or cemented medium. To make it compatible with the behaviour of overconsolidated soils and soft rocks, we propose to make  $\varphi'$  tend towards a value of  $\alpha$  so that  $\alpha = 1 - \pi \cdot \varphi' / 180$ , which amounts to express:

Figure 5. Dimensionless PMT chart based on state parameters  $E_M/p_{LM}^*$  and  $p_{LM}^*/p_0$ , comprising isolines of the values for  $\alpha$  (Eq. 3) and the estimation for  $\varphi'$  (Eq. 9).

## 6. Correlation between PMT results and drilling parameters.

Several PMT surveys have been made using the method of self-boring slotted tube with the special drilling rig Rotostaf (Arsonnet et al. 2013) allowing simultaneous rotation and penetration of the open end slotted casing, and evacuation of sediments inside the casing.

Records of drilling parameters of the rig can be interpreted to furnish (Baud, 2018):

- A parameter of drilling energy  $E_F$  (joules):

$$E_{F(j)} = \left(1 + \frac{1 \text{ atm}}{(1 \text{ atm} + P_I)}\right)^{1/2} \left(\frac{P_O \cdot C_R \cdot}{m \cdot (V_A/t)}\right)^{1/2} \quad (10)$$

whith drilling acceleration  $V_A/t$  (m/s<sup>2</sup>), torque  $C_R$  (N.m), tool thrust  $P_O$  (N), injection pressure  $P_I$  (atm), drilled ground mass  $m$  (kg).

- With adjunction of the ratio  $V_R/V_A$  of the rotation speed  $V_R$  versus drilling advancement speed, and a drill tool wear index based on a measurement of actual diameter of the Staf tool  $D_{mm}$ , a global parameter  $M$  (joules) is calculated, aiming a correlation with Ménard  $E_M$  modulus:

$$M_{Ménard} = \left\{ [\pi \cdot (D_{mm} - 63 \text{ mm})] \cdot \frac{V_R}{V_A} \cdot \left(1 + \frac{1 \text{ atm}}{(1 \text{ atm} + P_I)}\right) \cdot \left(\frac{P_O \cdot C_R \cdot}{m \cdot (V_A/t)}\right) \right\}^{1/2} \quad (11)$$

In the drilling and testing log in Fig. 6 are reported the results of a PMT profile in dune sands at Messanges (Landes, France) made in the frame of ARSCOP (Arscop, 2019) by self-boring of slotted casing, with PMT tests between 3 and 10m depth, using a Rotostaf drilling rig. This log shows the fairly good correlation of  $E_F$  and  $M_{Ménard}$  (in MJ, megajoule), respectively with  $p^*_{LM}$  and  $E_M$  (in MPa, megapascal).

The same set of results are reported in the adimensional diagram (Fig. 5):

- Drilling parameters, averaged each centimeter depth, by  $E_F$  as abscissa and  $M/E_F$  as ordinate.
- The 8 Pressurimeter tests by  $p^*_{LM}/p_0$  as abscissa and  $E_M/p^*_{LM}$  as ordinate.

In other words,  $(V_R/V_A)^{1/2}$ , known from long time as Somerton index, (Somerton, 1950) is more or less of the same nature, for soils in which is made drilling, than  $E_M/p^*_{LM}$  ratio.

Then, the  $\alpha$  rheological coefficient of Ménard can be estimated by this other approach, by complete interpretation of drilling parameters. In this example, all results are included in the range  $\alpha=1/3 \pm 15\%$ , which is a classical  $\alpha$  value representative for sands.

This underlines the need to systematically record the speed of rotation when drilling. The current recordings reduced to drilling speed  $V_A$  and only 3 pressures on the hydraulic and injection circuits of the rig furnish only partial data, not sufficient to anticipate soil behaviour and classification from drilling records.

It should be noted that this correlation has so far not been completely extended to drilling prior to PMT testing by conventional OHDM (open-hole drilling with mud) or RPM (rotopercussion with mud), two techniques commonly used for PMT drilling. Nevertheless, the continuous line drawn in such cases on the adimensional chart remains clearly representative of an evolution of the lithological profile crossed by the borehole ; more dispersion of PMT results are often related to decompression before time of testing.

Reiffsteck et al. (2016) demonstrated that it was possible to build a soil classification with basic drilling parameters expressed in terms of normalised friction  $Fr$  and normalised penetration rate  $Qr$ . The graphical report is more similar to Robertson than to Pressiorama charts, but is based on the same approach of combining a failure parameter and a deformation parameter with a range of behaviours from granular soils to coherent soils.

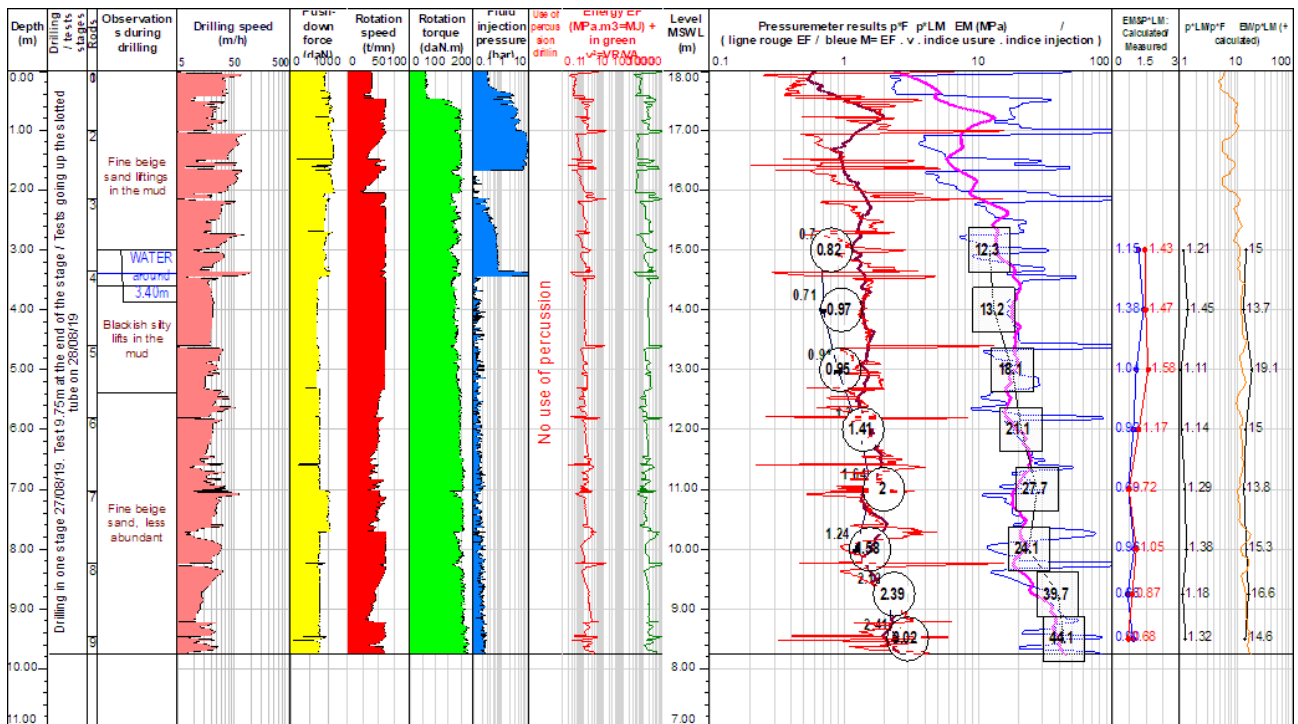


**Figure 6.** An example of interpretation of drilling parameters during self-boring of slotted casing together with the PMT tests made inside (Staf method).

## 7. Pressiorama® Chart based on one-cycle PMT

Determination of a value for  $\alpha$  from only measurements linked to the test,  $p^*_{LM}$ ,  $E_M$ , and the earth pressure at rest  $p_0$  at test depth, brings extended possibilities to get more from each test. But a better way than calculation to get  $\alpha$  is to measure it. The original definition (Ménard & Rousseau 1961, TLM 1963) derives  $\alpha$  from  $E_a$  modulus of tests after 3 cycles:

$$\alpha \cong \left(\frac{E_M}{E_a}\right)^{1/2} \quad (12)$$

It can be simplified due to the fact that stabilised cyclic modulus is almost get from a single loop with the approximation  $E_{c1} \cong 0.9 E_a$ , so:

$$\alpha = \left(0.9 \frac{E_M}{E_{c1}}\right)^{1/2} \quad (13)$$

A new sketch of Pressuremeter classification can be made by drawing for PMT as x-axis the ratio  $E_{c1}/E_M$  and as y-axis the main pressiometric state parameter  $p^*_{LM}/p_0$ . This new Pressiorama® cyclic chart (Fig. 7) brings a better space for dispatching soil and rock classification from tests results.  $p^*_{LM}/p_0$  axis is down positive, so that rocks are at the base and soils

overliethem, up to loose soils at top of the graph, as an image of drilling logs in nature. Other axes can be drawn:  $\alpha$  as secondary x-axis by Eq. (13), and consequently  $E_M/p_0$  and  $E_M/p^*_{LM}$  from Eq. (3).

The relation given in Eq. (7bis) between  $p^*_{LM}/p_0$  and  $\phi'$  can be written using directly  $E_M$  and  $E_{c1}$

$$\frac{p^*_{LM}}{p_0} = 0.1 \frac{E_M}{E_{c1}} \cdot e^{\frac{\phi'}{6}} \quad (14)$$

With the same assumptions than for Eq. (8) making asymptotic lines parallel to  $\alpha$  abscissas for hard soils and soft rocks, we get a complete, rather no so simple, expression of  $\phi'$  for tests with one unload-reload loop:

$$\phi' = 3 \cdot \ln \left( 10 \cdot \frac{E_{c1}}{E_M} \cdot \frac{p^*_{LM}}{p_0} \right) + \frac{90}{\pi} \left( 1 - \left( 0.9 \frac{E_M}{E_{c1}} \right)^{1/2} \right) \quad (15)$$

In Fig. 7, cases of cyclic tests in soils whose  $\phi'$  values can be measured or estimated by other ways had been checked to fix values of a, b and c in Eq.7 to obtain Eq.8. Similarly, we modified the expression of a ranking coefficient  $I_c$  proposed by Reiffsteck et al. (2013) to bring it to describe the space between 1 (minimum) for pure clay and 4 (maximum) for gravelly soils:

$$I_c = [\ln(p^*_{LM}/p_0) + (1 + \ln(E_M/E_{c1}))^2]^{1/2} \quad (16)$$

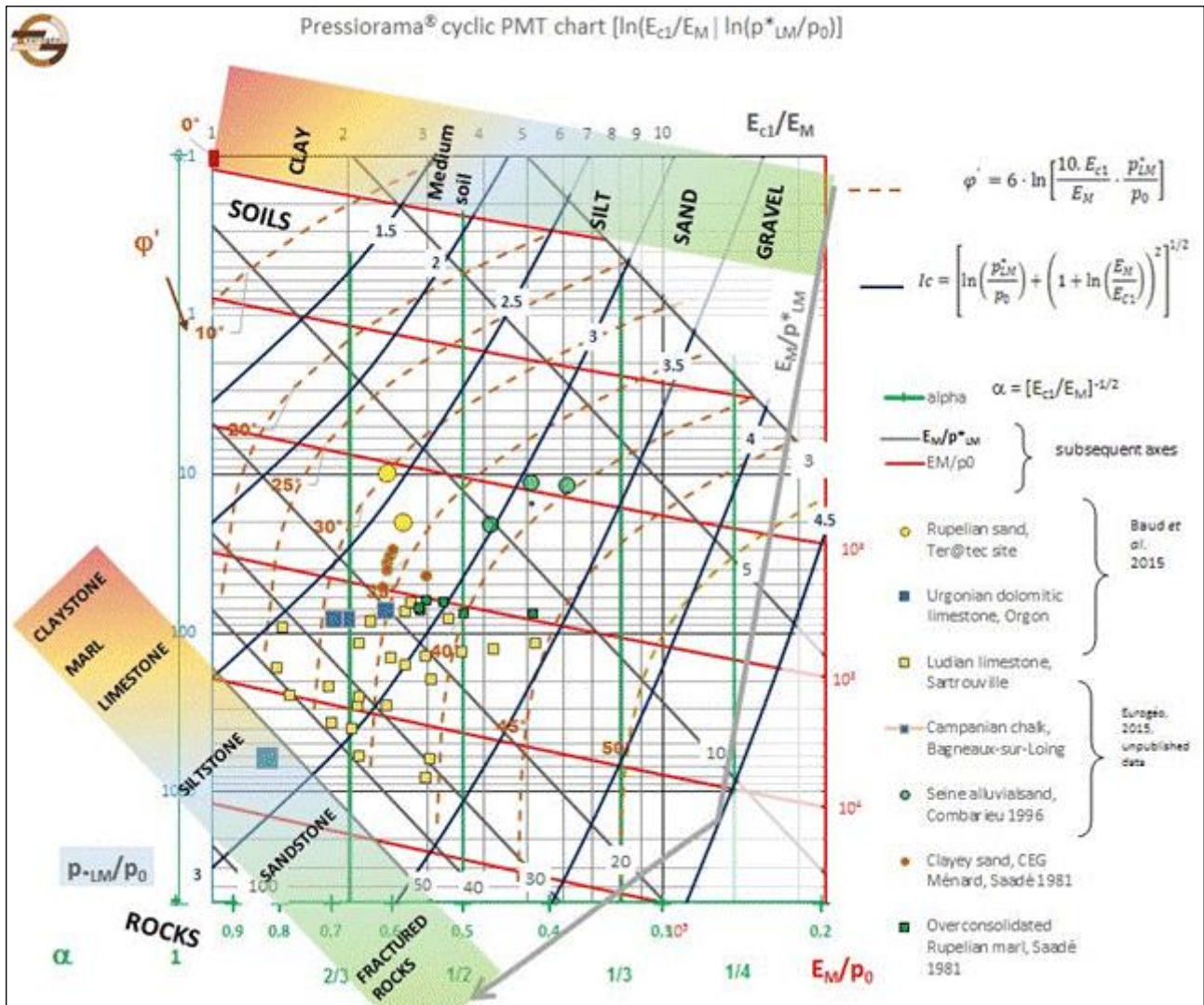


Figure 7. Soils and rocks classification from cyclic PMT

Ic values around 2.5 to 3 corresponding to the silts ensure the border, if any, between cohesive soils and granular soils. It is notable that, for low values of  $p_{LM}^*/p_0$  i.e. soft soils, this index Ic is approximately equal to  $1/\alpha$ . As the soil consolidation progresses, that is to say the three state parameters ( $p_{LM}^*/p_0$ ,  $E_M/p_0$ ,  $E_M/p_{LM}^*$ ) are simultaneously increasing, soil index Ic drifts to higher values of the rheological coefficient  $\alpha$ . This index seems a good descriptor of the more cohesive nature of the soil, or more granular. Other observations trend to the adequacy of this index with soil lithology, among the case histories used in the chart, and others. Nevertheless, more cases must be checked to improve this chart, and for that Ménard PMT have to be performed more currently with one cycle (according to ISO 22476-5). Just as for initial  $[E_M/p_{LM}^* | p_{LM}^*/p_0$  or  $p_{LM}^*/p_0]$  diagrams, too remoulded tests, even with one cyclic loop, trend to give underestimation of  $E_M$ , so underestimation of  $E_M/p_{LM}^*$  and overestimation of  $E_{C1}/E_M$ , and consequently low value for  $\alpha$  and high value for Ic : in other words, remoulded soil trends to appear as granular soil, and this is truly conform, the decompressed or disturbed soil is sheared in elements that make it appear falsely granular, and must be corrected by a decompression parameter as proposed in Fig.1.

## 8. Conclusions

The Pressiorama diagram was originally designed to quickly give a global view of the range of classical characteristics,  $E_M$  modulus and  $p_{LM}^*$  limit pressure, obtained in a series of pressuremeter profiles at a given site. It has led to successful applications in many areas of geotechnical works in soils and rocks. This diversity of applications only reflects the soil characterization power provided by Louis Ménard's invention of his Pressuremeter, and of design methods that he quickly founded between 1955 and 1970, for which the concept of rheological coefficient specific to each type of soil is a basic component.

Our current research is just another presentation of these dazzling intuitions. Applications have been exposed here in the fields of geomechanical classification of soils and rocks, of earthworks and drilling works, of the correlation with the classical mechanical characteristics of the ground, and of seismic zoning.

Nevertheless, for a systematic use of the charts presented here, it is recommended and essential to bear in mind that they should only be applied to tests perfectly executed in the rules of art, and for which it is certain that they are representative of the ground under test. This is obtained by controlling the degree of decompression of the soil before the test, and getting the most accurate knowledge possible of the nature and structure of the ground, by careful examination of drill cuttings, their identification and their place in the geological context of the surveyed site, for which a reliable geotechnical stratigraphic column must be established.

## Acknowledgements

The author wishes to thank Michel Gambin for its leading role in the development of Pressiorama® charts since

their origin, and the assurance he gave us to continue the momentum of Pressuremeter by Louis Ménard. These acknowledgements also go to owners who accepted the use and publication of PMT from their survey sites, and to experienced geotechnical engineers in theory and practice of Pressuremeter, who encouraged this graphical geological approach, particularly O. Combarieu, C. Dalton, R. Frank, J.-P. Magnan, J. Monnet, F. Schlosser, and A. Viana da Fonseca.

## References

- [1] AFNOR NF EN ISO 22476-4 « Essai au pressiomètre Ménard », Mai 2015
- [2] ARSCOP “Projet National nouvelles Approches de Reconnaissance des Sols et de Conception des Ouvrages géotechniques avec le Pressiomètre” (French National Project New Approaches to Soil Investigations and Design of Geotechnical Structures with the Pressuremeter). Internal report C. Jacquard “Essais croisés Messanges” (oct.2019) (in French)
- [3] Baguelin F., Jézéquel J-F., Shields D.H. (1978). “The Pressuremeter and foundation engineering”. Clausthal, Germany. Trans Tech Publications
- [4] Baud J.-P. (2005) “Analyse des résultats pressiométriques Ménard dans un diagramme spectral  $[\text{Log}(p_{LM}), \text{Log}(E_M/p_{LM})]$  et utilisation des regroupements statistiques dans la modélisation d’un site” (A  $[\text{Log}(p_{LM}), \text{Log}(E_M/p_{LM})]$  diagram for spectral analysis) of Ménard pressuremeter tests results. Application to geotechnical site surveys) In: Gambin, Magnan, Mestat (eds.), 5<sup>th</sup> International Symposium on Pressuremeter, 50 ans de pressiomètres, ISP5-PRESSIO 2005, vol 1. Presses ENPC, Paris, France, 2005, pp 167–174 (in French) [English version available from author]
- [5] Baud J.-P. (2016) “Apport de l’essai cyclique à la classification pressiométrique des sols et des roches” (Improvement of soils and rocks classification by pressuremeter cyclic tests), In: Journées Nationales de Géotechnique et de Géologie de l’Ingénieur, JNGG 2016 Nancy, France, 2016 (in French). [http://www.eurogeo.eu/CMS/modules/dl/759056071/Baud\\_sciences-conf.org\\_jngg2016\\_81625\\_V12.pdf](http://www.eurogeo.eu/CMS/modules/dl/759056071/Baud_sciences-conf.org_jngg2016_81625_V12.pdf)
- [6] Baud J.-P. (2018) “Corrélation entre paramètres de forages et profils pressiométriques par autoforage du tubage Rotostaf” (Correlations between drilling penetration and PMT logs when using slotted casing emplaced by Rotostaf self-boring), In: Journées Nationales de Géotechnique et de Géologie de l’Ingénieur, JNGG2018, Champs-sur-Marne, France, 2018 (in French)
- [7] Baud J.-P., Gambin M. (2013) “Détermination du coefficient rhéologique  $\alpha$  de Ménard dans le diagramme Pressiorama®” (Obtaining the Ménard  $\alpha$  Rheological Factor in a Pressiorama® Diagram), Actes du 18ème CIMSG, Proc.18th Intl. Conf. Soil Mech. and Geotech. Eng., Paris, France, 2013 (in French) [Oral presentation slides in english available from the authors]
- [8] Baud J.-P., Gambin M. (2014) “Soil and Rock Classification from High Pressure Borehole Expansion Tests”, Springer, Geotech. Geol. Eng. (2014) 32 pp1397–1403
- [9] Baud J.-P., Gambin M., Heintz R. (2015) “Modules élastiques, pseudo-élastiques et cycliques dans l’essai pressiométrique Ménard : historique et pertinence actuelle” (Ménard Pressuremeter modulus: Relationship and correlations between elastic, pseudo-elastic and cyclic E-modulus as defined by Louis Ménard) In : Frikha, Varaksin, Gambin (eds.) ISP7 - PRESSIO 2015, Hammamet, Tunisie, 2015, pp 317-327 (in French) [English version available from authors]. [https://www.geotech-fr.org/archives-congres-internationaux/ISP7/2015/details \(session 3, #9\)](https://www.geotech-fr.org/archives-congres-internationaux/ISP7/2015/details(session%203,%20#9))
- [10] Caterpillar Inc. (from 1960’s, updated), “Caterpillar Performance Handbook”, Ed.29, pp 69-76. [http://nees.ucsd.edu/facilities/docs/Performance\\_Handbook\\_416C.pdf](http://nees.ucsd.edu/facilities/docs/Performance_Handbook_416C.pdf)
- [11] Combarieu O. (1996) “A propos de la détermination de l’angle de frottement des sols pulvérulents au pressiomètre”. Rev. Fr. Géotechnique, 77, pp 51-57 (in French)
- [12] Combarieu O., Canepa Y. (2001) “L’essai cyclique au pressiomètre,” Bull. Liaison des P. & C., n° 233, pp 37-65 (in French)
- [13] Dupla J.-C., Canou J. (2005) “Paramètre d’état des sables et essai pressiométrique”. In: Gambin, Magnan, Mestat (eds.) ISP5-PRESSIO 2005, vol 1. Presses ENPC, Paris, pp 255-265 (in French)

- [14] Elfatih M.A., Mohamed A.O., Mouhanad A. (2015) Use of the Ménard Pressuremeter for the characterization of Nubian sandstone of Sudan. In: Frikha, Varaksin, Gambin (eds.) ISP7 - PRESSIO 2015, Hammamet, pp 395-401. [https://www.geotech-fr.org/archives-congres/congres-internationaux/ISP7/2015/details \(session 5 #2\)](https://www.geotech-fr.org/archives-congres/congres-internationaux/ISP7/2015/details(session%205%20#2))
- [15] Gambin M. (1977) "Le Pressiomètre et la détermination de l'angle de frottement et de la cohésion d'un sol". Colloque de Halin (Pologne) 25 ans Geoprojekt (in French)
- [16] Hamidi B., Nikraz H., Yee K., Varaksin S., Wong L.T. (2010) "Ground Improvement in Deep Waters Using Dynamic Replacement", Proceedings of the 20th International Offshore and Polar Engineering Conference, Beijing, China, June 20-25, 2010, pp 848-853
- [17] Hamdi S., Holeyman A. (2016) "Numerical modelling of cylindrical cavity expansion in rock mass based on the Hoek-Brown yield criterion" Pre-print, Springer Journal: Innovative Infrastructure Solutions (under press)
- [18] ISO ISO/FDIS 22476-4:2021(E) "Prebored pressuremeter test by Ménard procedure". Final draft under voting process, 2021.
- [19] ISO ISO-TC182-WG8\_N34\_prEN\_ISO\_22476-5 "Geotechnical investigation and testing - Field testing - Part 5: Prebored pressuremeter test" WG8 Working Document, J. Habert, convenor, *et al.*, 2021
- [20] Kanji M.A. (2014) "Critical issues in soft rocks", Journ. Rock Mechanics and Geotechnical Eng. 6 – 2014, pp 186-195. Elsevier & Institute of Rock and Soil Mechanics, Chinese Academy of Sciences. <http://www.sciencedirect.com/science/article/pii/S1674775514000389>
- [21] Martí Armengola X., Pérez García N., Devincenzia M. (2019) "Uso del Presiómetro en la caracterización de las margas de la formación Madingo (Use of pressuremeter test in the Madingo formation marls characterization)", Geotecnia n° 147 – nov.2019 – pp. 15-25. <http://doi.org/10.24849/j.geot.2019.147.02> (in Spanish)
- [22] Ménard L. (1957) "An apparatus for measuring the strength of soils in place", Thesis for the degree of Master of Science, University of Illinois, USA, 1957
- [23] Ménard L. & Rousseau J. (1961) "L'évaluation des tassements, tendances Nouvelles" (Settlements evaluation, new trends) Sols-Soils, n°1, Paris, 1961 (in French)
- [24] Monnet J., Khelif J., (1997) "Etude théorique de l'équilibre élastoplastique d'un sol pulvérulent autour du pressiomètre" () Rev. Fr. Géotechnique, 77, pp 3-12 (in French)
- [25] Monnet J. (2013) "Caractérisation mécanique des sols par l'essai pressiométrique". 18ème CISMIG, Paris 2013. ISP6 Parallel session. (in French)
- [26] Müller H. (1970) "Baugrunduntersuchung mit der Pressiometerverfahren nach Ménard" (Subsoil investigation with Ménard pressuremeter method), Die Bautechnik, Berlin, Heft 9, pp 289-295 (in German)
- [27] Reiffsteck P., Martin A., Périni T. (2013) "Application et validation d'abaque pour la classification des sols à partir des résultats pressiométriques", Actes du 18ème CISMIG, Proc.18th Intl. Conf. Soil Mech. and Geotech. Eng., Paris, Parallel session ISP6/#4-6 (in French)
- [28] Reiffsteck P., Benoit J., Hamel M., Vaillant J.M. (2016) "Proposition d'une méthode de classification basée sur les paramètres de forage". JNGG, Nancy (in French) <https://jngg2016.sciences-conf.org/browse/session?sessionid=1215>
- [29] Ritsos A., Basdekis A., Gambin M. (2013) "Pressiorama - Application of Ménard Pressuremeter to classify several geological formations encountered in Greece". Proc.18th Intl. Conf. Soil Mech. and Geotech. Eng., Paris, Parallel session ISP6/#4-7
- [30] Salençon J. (1966) "Expansion quasi-statique d'une cavité à symétrie sphérique ou cylindrique dans un milieu élastoplastique". Paris, Ann. Ponts et Chaussées, III, 175-187 (in French)
- [31] Saadé C. (1981) "Essais pressiométriques et essais cycliques". Mémoire D.E.A., Ecole Centrale des Arts et Manufactures, Sèvres (in French)
- [32] Somerton W.H. (1959) "A laboratory study of rock breakage by rotary drilling". Petroleum transactions, AIME, 216, p. 92-97.
- [33] Tarnawski M., Ura M. (2015) "Towards soil profile from pressuremeter data". In: Frikha, Varaksin, Gambin (eds.) ISP7 - PRESSIO 2015, Hammamet, pp 281-288. [https://www.geotech-fr.org/archives-congres/congres-internationaux/ISP7/2015/details \(session 3 #5\)](https://www.geotech-fr.org/archives-congres/congres-internationaux/ISP7/2015/details(session%203%20#5))
- [34] Techniques Louis Ménard (1963) "Détermination de la poussée exercée par un sol sur une paroi de soutènement." Notice D38 (révision 1970) CEG Ménard Paris (in French)
- [35] Techniques Louis Ménard, (1963) "Règles d'utilisation des techniques pressiométriques" (in French) "The Ménard Pressuremeter - Interpretation and application of Pressuremeter tests results to foundation design" Ménard General Memorandum D60, CEG Ménard Paris (editions up to 1982). [Paper or e-copy available from the author]